García Baldoví, H.; Víctor, VM.; Herance Camacho, JR.; Alvaro Rodríguez, MM.; García Gómez, H. (2015). Perylenetetracarboxylic anhydride as a precursor of fluorescent carbon nanoonion rings. Nanoscale. 7(29):12484-12491. doi:10.1039/C5NR02903A.

Perylenetetracarboxylic anhydride as precursor of fluorescent carbon nanoonion rings.

Herme G. Baldoví,[a] José Raul Herance,[1a,b] Víctor Manuel Víctor,[b,c,d] Mercedes Alvaro,[a] and Hermenegildo Garcia[*,a,e]

Thermal annealing at 400 ºC of perylenetetracarboxylic anhydride in low molecular mass PEG gives rise to the formation of well defined nanoobjects of 2.5 nm height and size distribution from 10 to 65 nm (average 40 nm) after purification of the raw mixture with silicagel chromatography. TEM reveals that the flat nanoobjects are constituted by concentric graphenic rings (0.34 nm interlayer distance). The morphology of the nanoparticles resembles onion rings of nanometric dimensions (nanoonion rings C-NOR). C-NOR particles have an excitation dependent emission with λ_{em} from 430 to 570 nm and maximum emission quantum yield of 0.49. C-NOR particles can be internalized inside Hep3B human hepatoma cells as determined by confocal fluorescence microscopy and are remarkably biocompatible affecting slightly to cell viability according to MTT test.

INTRODUCTION.

There is much current interest in the synthesis of fluorescent carbon-based nanoparticles (C-dots) and other carbon nanoforms that can replace quantum dots for bioimaging and other applications avoiding the use of toxic metals and increasing biocompatibility.[1 2] Most of the reports on the preparation of fluorescent C-dots employ organic precursors that contain non-aromatic sp^3 carbon atoms.[2-6] Thermolysis of polyethylene glycol (PEG) at temperature of 400 ºC has been reported to be sufficient to generate C-dots.[7-10] In other reports, PEG is used as additive in the preparation of fluorescent C-dots to cover and protect their surface, resulting in an increase of the emission intensity.[11-13] Studies describing aromatic compounds as precursors of C-dots are much scarcer. [1 2 14] Aromatic compounds as precursors of C-dots can, in principle, offer a prearrangement of the carbon atoms in a rigid molecular environment that could be preserved during the thermolysis leading to the formation of the C-dot. In addition, the rigidity of aromatic compounds if suitably transferred to the resulting C-dot could be very interesting to increase the emission quantum yield by disfavouring non emissive deactivation pathways based on conformational relaxation of the excitons.

In the present manuscript we report that perylenetetracarboxilic anhydride (PTA) is a suitable precursor of C-nanoonion rings (C-NORs) with well defined and extremely uniform morphology and high emission efficiency that can be useful for bioimaging considering that they exhibit a high biocompatibility.

RESULTS AND DISCUSSION.

C-NORs were prepared from PTA (see molecular structure in Scheme 1). The procedure involves dissolving PTA in low-molecular mass PEG (M<400 Da) that is introduced in an oven preheated at 400 ºC and, then, the oven switched off and mixture cooled down by exposure to the ambient (about 20 h). Two samples obtained under the same conditions, but in the absence or presence of $Eu(OAc)_3$ as Lewis acid to promote the reaction of the anhydride functional groups of PTA and the carboxylic acids generated from them with the hydroxyl groups of PEG, were prepared, rendering the samples C-NOR and C-NOR(Eu) depending on the absence or the use of Eu in the synthesis. In the literature there several examples showing that rare earth metal ions can act as Lewis acid esterification catalysts and the same function was expected here.[15,16] The selection of $Eu(OAc)_3$ was also based on the possibility to detect the presence of Eu^{3+} in the sample by observing the characteristic photoluminescence of this lanthanide.[17-19] In comparison the use of ZnCl2 as Lewis acid to promote PEG esterification renders under the same conditions crude mixtures considerably more black, but where also C-Nor were observed. After formation of C-NORs, purification from the black viscous PEG media was carried out by conventional silica gel chromatography using acetonitrile as eluent, following the fractions during purification by fluorescence. Although nanoparticles are not commonly purified, we have observed that, at least in the present case, chromatography is a suitable technique to select C-NOR with narrower particle size distribution. The selection of acetonitrile as eluent of the preparative chromatography was made based on the elution of the crude mixture in thin layer chromatography. The present procedures was found to provide reliable C-NOR nanobjects with consistent morphology and properties in a reliable and reproducible manner. Scheme 1 summarizes C-NOR preparation procedure.

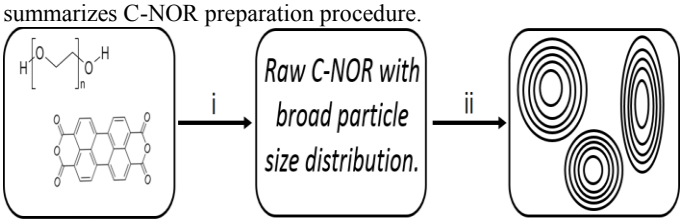

Scheme 1. Preparation procedure for C-NOR. i) Treatment in a oven preheated at 400 ºC and slow cool down to room temperature by exposure to the ambient (20 h) and ii) purification of the black viscous mixture by silica gel chromatography.

Comparison of C-NORs before and after purification reveals that the consequence of the purification is a narrower particle size distribution of the purified C-NOR fraction compared to the raw mixture (see Figure 1). It could even be that more appropriate selection of the stationary mobile phase could results in an even narrower particle size distribution. In fact the nanometric dimensions and the onion ring morphology of the material derived

from the thermal treatment of PTA were determined by transmission electron microscopy (TEM, see Figure 1, part b) that also allows establishing the particle size distribution. From these TEM images, the interlayer distance of 0.34 nm for the onion rings was determined (see panel d in Figure 1). This interlayer space corresponds to the spacing of graphene sheets in graphite and this value rules out that PEG could be present within the interlayer space of C-NOR. Identical nanoobjects were obtained when the synthesis was carried out in the presence of $Eu(OAc)_3$ or $ZnCl_2$.

Considering the use of PTA as precursor of C-NORs, formation of these nanoobjects can be rationalised as indicating the stacking by π–π interactions of PTA molecules in a concentric manner, resulting in the formation of quasi-circular or elliptical objects. The height of C-NORs was determined by AFM measurement that allows subnanometric vertical resolution (Figure 2). These AFM measurements show that the height of those nanoobjects about 2.5 nm is very homogeneous.

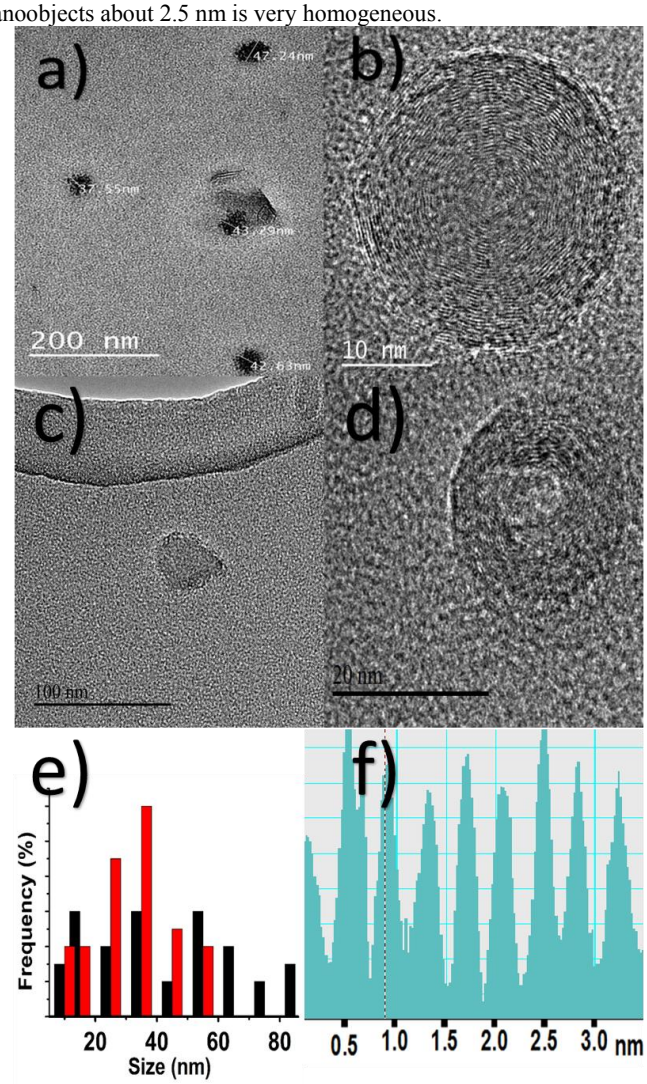

Figure 1. Selected TEM images of C-NOR (panels a and b) and C-NOR(Eu) (panels c and d) at two different magnifications. Panel e: statistical particle distribution of C-NOR before (black) and after (red) silica gel column chromatography. Panel f: Measurement of the interlayer distance for the C-NOR particle shown in panel b and corresponding to the value expected for the interlayer distance in graphite materials.

This height value is larger than that estimated for PTA based on molecular mechanics (larges axis 1.15 nm) and accordingly it seems that the present thermal treatment in PEG leads to the assembling and the π–π stacking of PEG-modified PTA units that should have larger dimensions than PTA itself. Related to the present findings, it has been reported in the literature that extremely high pressures (8 GPa) and temperatures (1300 ºC) over perylene samples leads to the formation of diamond particles impurified by the presence of small percentage of carbon nanoforms including onion spheres (15-30 nm size) and accompanied with particles of similar morphology to graphitic ribbons.[20-24] It was observed that under these extremely high pressure conditions most of the condensed aromatic compounds from naphthalene, anthracene, pentacene and coronene render

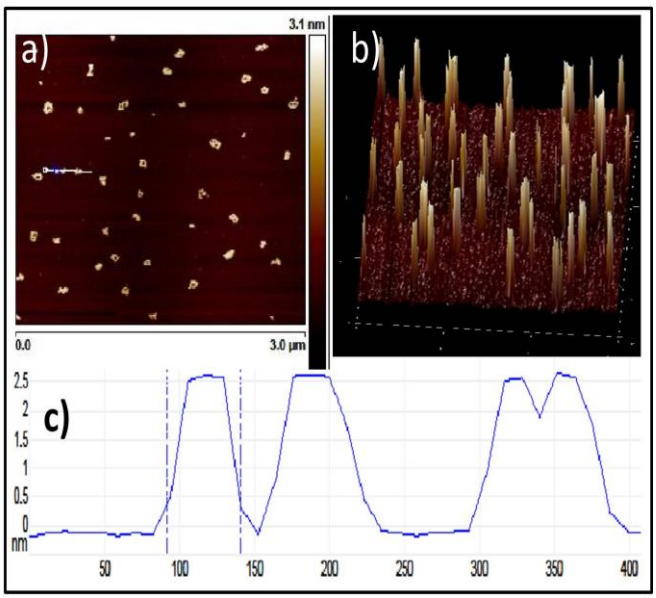

Figure 2. Two views of a representative AFM image of C-NOR nanoobjects after chromatographic purification in which the presence of highly homogeneous particles with regard to their height can be seen.

besides diamond a small proportion of nanometric particles of similar type as C-NOR here characterized by TEM and AFM, except that in the precedent the shape of the material was assumed to be spherical based on TEM images. Similar nanoonions have also been characterised in experiments performing graphite melting at ultrahigh pressure and temperature (5-30 GPa, 5000-6000 ºC), or in flame or by high power laser pulse.[25-27] It seems that the thermal treatment in PEG performed here causes an assembling process resulting in analogous nanoobjects, but taking place under our much milder conditions.

One of the most interesting properties of C-dots and other carbon nanoforms is the observation for these nanoparticles of an intense photoluminescence.[1,7,28,29] In the present case, no studies on the photoluminescence of onion-like carbon nanospheres have been reported. In our case, we were interested in this property considering the potential use of carbon nanoforms in imagining especially for biological systems. Aimed at studying the photoluminescence of C-NOR, the UV-Vis absorption spectrum of purified C-NOR and C-NOR(Eu) was initially recorded (Figure 3).

As it can be seen in this Figure 3, the UV-Vis spectra of C-NOR and C-NOR(Eu) exhibit the presence of a distinctive

absorption band in the visible region (λ_{max}=440 nm) on top of an absorption background. Comparison of the shape and position of this visible band present in both C-NOR and C-NOR(Eu) indicates that it appears between the position of the visible absorption bands of PTA (λ_{max}=520 nm) and perylene (λ_{max}=420 nm), but lacking the fine vibrational band structure characteristic of these two polycyclic aromatic compounds (see also Figure 3). Considering the λ_{max} value measured for PTA and perylene, it could be that the absorption observed band of C-NOR and C-NOR(Eu) correspond to some PTA derivative formed in the thermal annealing. It seems, however, that the fraction exhibiting the characteristic 440 nm band is predominant under Lewis acid catalysis by Eu^{3+}, while it

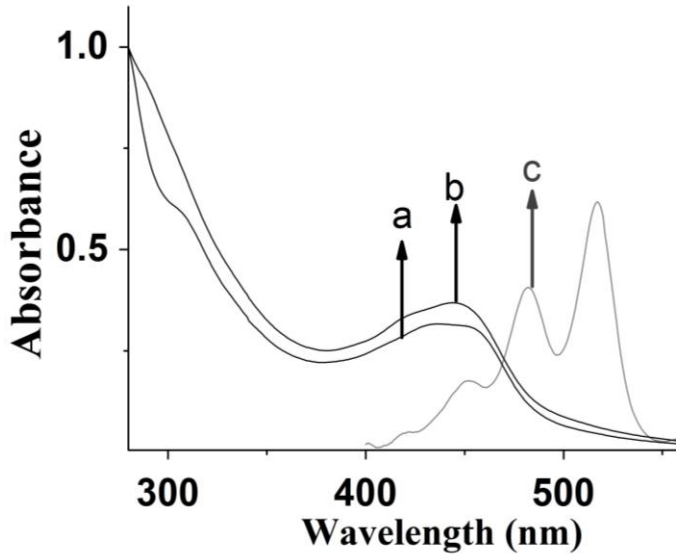

Figure 3. Absorption spectra of C-NOR (a), and C-NOR(Eu) (b) after chromatographic purification in comparison with the absorption spectrum of PTA (c) in acetonitrile.

is relatively minor in the raw mixture after PTA annealing under the conditions followed for the preparation of C-NOR, reflecting the influence of Eu^{3+} as Lewis acid in the thermal treatment, promoting acid catalyzed reactions probably between the anhydride group of PTA and hydroxyl groups of PEG. Particularly, carboxylic esters from partial decarboxylated PTA and PEG are potential candidates that can rationalise the λ_{max} value of the absorption band present in C-NOR and C-NOR(Eu).

Excitation of C-NOR and C-NOR(Eu) allows detection of a strong emission. Importantly, a shift in the position of the emission band depending on the excitation wavelength in the range 350-500 nm was observed.[4] This behaviour is considered as specific of C-dots and has been attributed to radiative electron/hole recombination at different sites, in C-dots having a distribution of trapping sites. In the present case the maximum emission intensity was recorded upon excitation of C-NOR and C-NOR(Eu) between 350 to 400 nm.

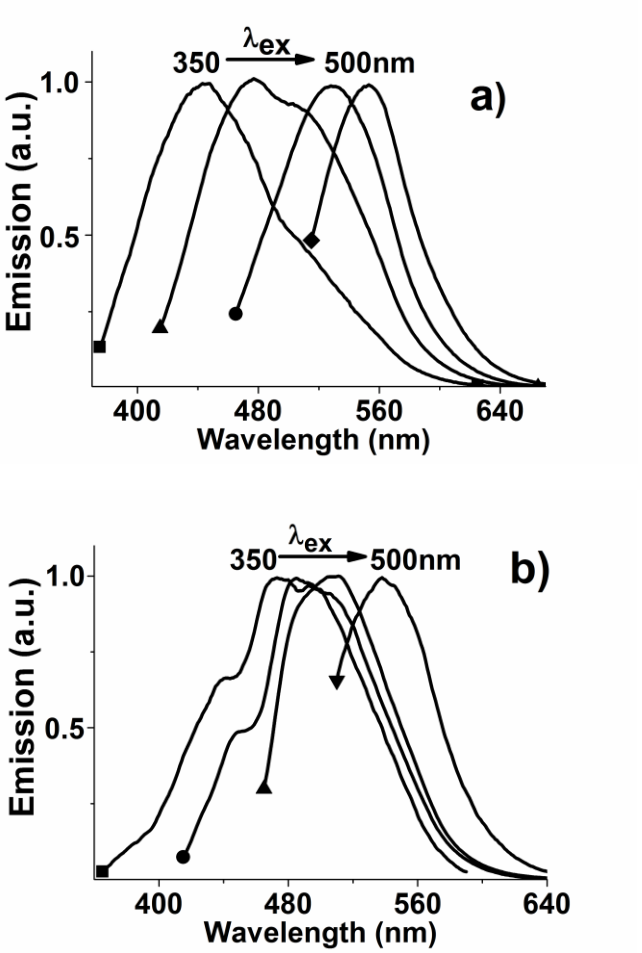

Figure 4. Normalised emission spectra of C-NOR (a) and C-NOR(Eu) (b) in acetonitrile solutions (λ_{ex}: 350 (■),400 (▲), 450 (●) and 500 (♦)).

Furthermore, one interesting point differentiating the emission from C-NOR and C-NOR(Eu) respect to PTA is the observation of the shift in the position of the λ_{em} upon excitation at different wavelengths and the almost complete disappearance of the vibrational structure present in the emission of PTA and is almost absent in the emission of C-NOR. We noted that excitation at 300 or 350 nm of this material presents one shoulder at the longer wavelength side. In the case of C-NOR(Eu), some vibrational structure although much less pronounced than for PTA is observed upon excitation at wavelengths between 300 and 400 nm. These features clearly rule out that the emission being observed for C-NOR is due to residual PTA as possible impurity present in the material. Also it should be commented that no evidence for atomic emission due to the Eu could be recorded for C-NOR(Eu) ant any excitation wavelength. This lack of Eu emission is in agreement with the absence of Eu in C-NOR(Eu) determined independently by ICP analysis.

The emission quantum yield (ϕ_{em}) of C-NOR and C-NOR(Eu) determined in methanol upon excitation of 350 nm were similar with values 0.47 and 0.49 for C-NOR and C-NOR(Eu), respectively. These ϕ_{em} compare favourably with most of the values reported in the literature for C-dots and are among the highest for this type of nanoobjects.[2] Emission lifetimes of C-NOR and C-NOR(Eu) upon 340 nm excitation were also similar for both samples, giving an estimated τ value obtained from the from best fit of the emission

temporal profile in acetonitrile to a first order decay of about 5.5 ns.

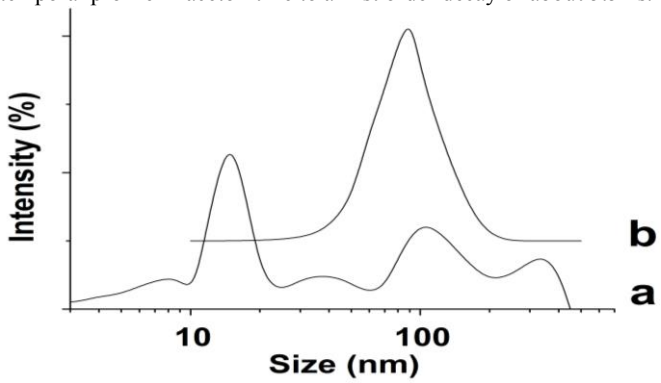

Figure 5. Dynamic laser scattering measured for C-NOR before (a) and after (b) purification.

Before chromatographic purification, the particle size distribution of raw C-NOR sample has at least five main components based on their analysis by dynamic laser scattering, the sizes ranging from less than 10 to 430 nm (Figure 5). The Z-potential, of this raw mixture was -16.4 mV, indicating that it is a relative instable colloidal dispersion. In contrast, after purification, the particle size distribution of the aqueous dispersion measured by dynamic laser scattering shows a single peak of 85 nm with a Z-potential of -29.5 mV, corresponding to a considerably more uniform distribution of more stable colloidal particles (Figure 5). We noted that the sizes of C-NOR in water measured by dynamic laser scattering were larger than those determined by HR-TEM, a fact that is commonly observed and is attributable to solvation of the nanoparticles and/or to the partial agglomeration of suspended particles. In addition it was also noticed that the more negative Z-potential of the purified C-NOR indicates the presence of a higher density of negative charges on the surface of C-NOR than the average for the raw mixture. Similar observations were also determined for the C-NOR(Eu) sample indicating that our silica gel chromatography is adequate to purify raw mixtures of C-NORs after thermal treatment.

After chromatographic purification, C-NOR and C-NOR(Eu) were characterised spectroscopically, both samples showing similar spectra. In IR spectroscopy the most intense absorption bands correspond to PEG appearing at 3500, 2950, 1480, and 1000 cm^{-1} attributable to the OH, CH_2 stretching, CH_2 bending and C-O vibrations, respectively. Thus, the most important information of IR is the presence of a high PEG content in C-NOR and C-NOR(Eu) samples. Besides PEG, both of C-NOR and C-NOR (Eu) exhibit weaker characteristic vibration bands corresponding to carbonyl groups about 1730 cm^{-1} attributable to carboxylic esters and 1610 cm^{-1} due to the stretching vibration of the aromatic rings (Figure 6) with minor differences in the position and peaks of low intensity between the two C-NOR samples.

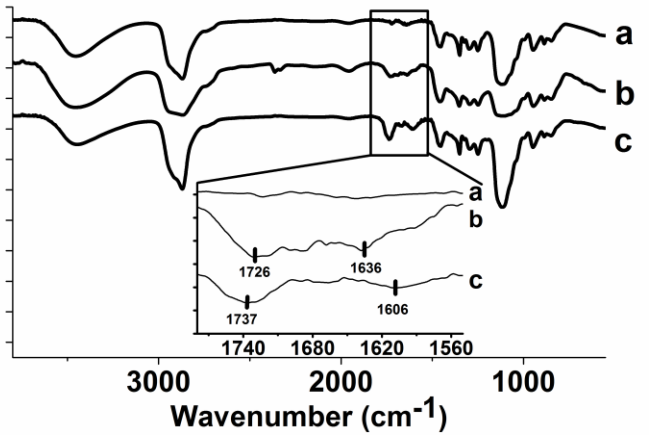

Figure 6. IR spectra of PEG (a), C-NOR (b) and C-NOR(Eu) (c). The inset shows and expansion of the C=O region showing the presence of vibration bands at different wavelengths in C-NOR (b) and C-NOR(Eu) (c) that are not present in PEG (a). The wavenumber values have been indicated in the inset.

The ^{1}H and ^{13}C NMR spectra of C-NOR samples and their interpretation as due to the combination of signals from PEG and PTA moieties are fully consistent with the previous IR spectra. Thus, besides a set of intense peaks corresponding to CH_2 groups of PEG about 3.5 ppm, ^{1}H NMR spectra recorded for C-NOR and C-NOR(Eu) in CD_3CN solution show in the aromatic region the presence of two doublets of doublets centred at 7.60 and 7.70 ppm corresponding to the aromatic protons derived from PTA. In ^{13}C NMR spectra the presence of a signal at 161 ppm corresponding to carbonyl carbons of carboxylic esters was recorded, indicating that the anhydride has been converted into ester groups during the thermal treatment with PEG.

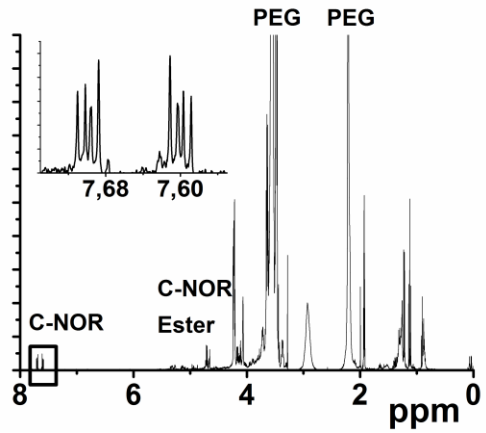

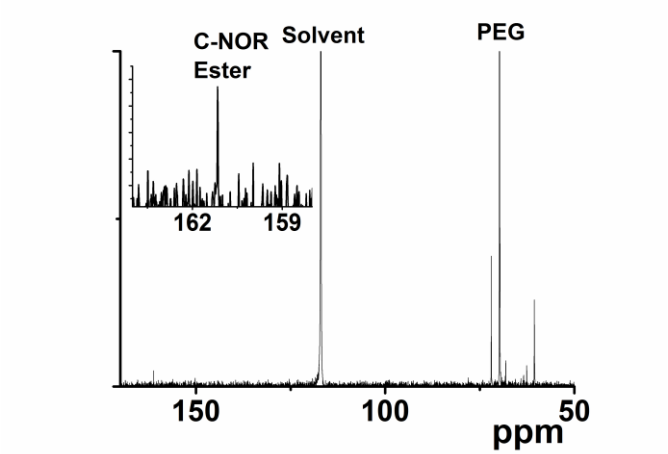

Figure 7. ^{1}H (a) and ^{13}C (b) NMR spectra recorded for C-NOR. Relevant peaks corresponding to PEG, solvent of C-NOR have been indicated in the Figure. The insets shows expansions of certain regions of the spectra.

Overall, the combination of the information provided by TEM with IR and NMR spectroscopy indicates that PEG must be capping and surrounding C-NOR and C-NOR(Eu), but PEG cannot be present inside the nanoparticles.

As commented in the introduction one of the main applications of fluorescence C-dots is bioimaging. Aimed at providing preliminary data showing the feasibility of application of C-NOR and C-NOR(Eu) in this field, preliminary tests showing biocompatibility of C-NOR and their ability to become internalized into cells were performed. Cell biocompatibility was determined for Hep3B cells that were grown for 3 h in a culture medium containing C-NOR and, then, grown for 24 h in its absence. Differences in cell activity between the controls and the Hep3B cells exposed to C-NOR were determined using the MTT activity test. MTT assay is based on the ability of living cells to reduce 3-(4,5-dimethylthiazol-2-yl)-2,5-diphenyltetrazolium bromide to formazan.[30-32] The test is based on the fact that this reduction indicates that reductase enzymes of mitochondria are active, reporting on biochemical activity of these key cellular organelles. The results are presented in Figure 8. As it can be seen there, a contact time of 3 h reduces slightly the cell viability respect to the control to 95% for C-NOR and to 90% in the case of C-NOR(Eu).

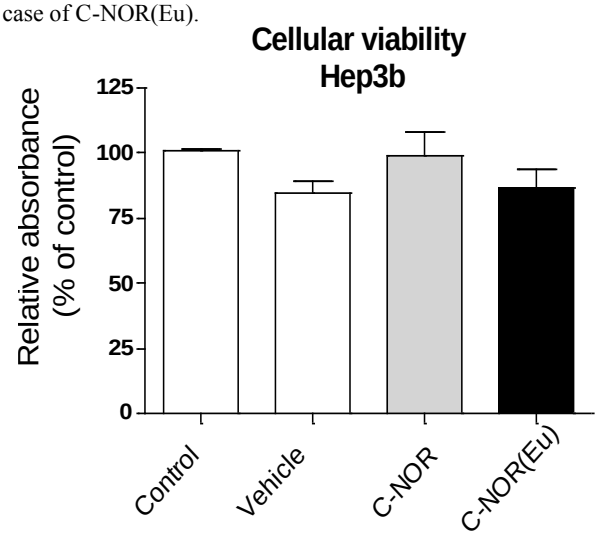

Figure 8. Cellular viability based in MTT assay of exponentially growing cells after 24 h of Hep3B cells culture exposed to C-NOR and C-NOR(Eu) for 3 h. Data (mean±S.E.M, *n*=5–6) were analyzed by Student´s t-test, significance vs control .

After having obtained data on the biocompatibility of C-NOR with Hep3B cells from human hepatocite, cells were cultured with C-NOR and C-NOR(Eu) for 24 h and, after this time, the cells were studied by confocal fluorescence spectroscopy trying to detect internalization of these fluorescent nanoobjects into cells. The results are presented in Figure 9, where a z-stacking of confocal images taken at about 1 μm increment in the vertical position are presented. The overlay of these images taken at about 1 μm of vertical offset allows obtaining firm tridimensional information from microscopy images. As it can be seen in Figure 8, the presence of green fluorescence corresponding to C-NOR at different Z ordinates clearly shows that both C-NOR and CNOR-(Eu) are able to permeate into cells.

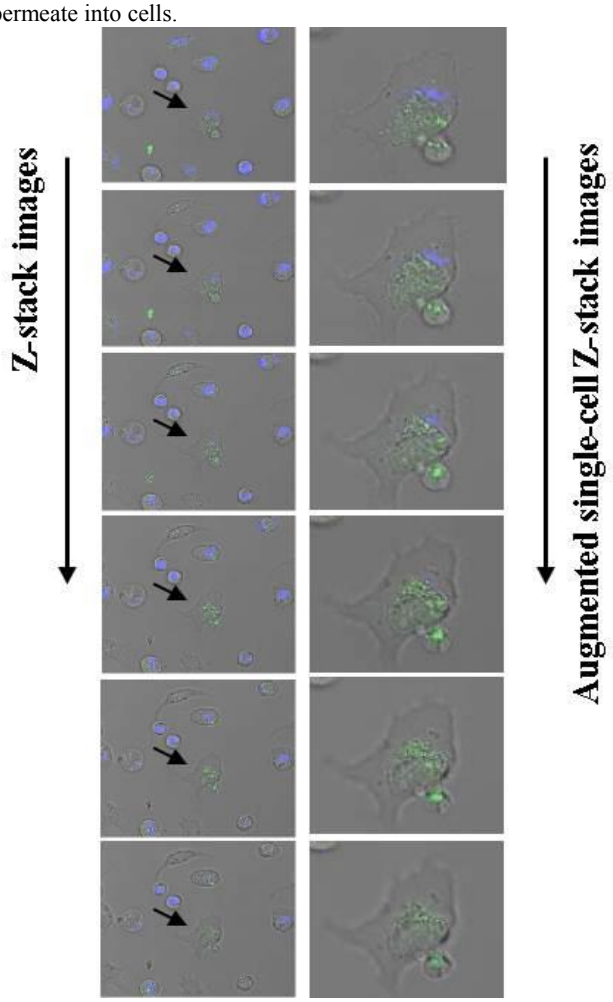

Figure 9. Vertical Z confocal images taken with overlay mode after exciting at 488 nm to show the location of C-NOR nanoparticles (green) in a Hep3B cell culture that have been stained at the nuclei with Hoechst dye (right panel from Z1 to Z6, 1.18 ±0.2 μm increment from top to bottom) and augmented single cell images (left panel from Z1 to Z6, 1.18 ±0.2 μm increment from top to bottom). The arrow points the augmented single cell selected for the Z-stack measurements. The blue color is due to the Hoescht dye locating the cell nuclei.

EXPERIMENTAL SECTION.

C-NOR and C-NOR(Eu) preparation. 100 mg of a commercial PTA (Sigma-Aldrich, CAS Number: 128-69-8) were suspended in 8 mL of PEG 400 (Fluka Analytical, Mr = 380-420 g/mol, CAS Number:25322-68-3) in the absence (C-NOR) or containing 100 mg of $Eu(OAc)_3 \bullet 3H_2O$ (Sigma Aldrich, CAS Number: 62667-64-5, C-NOR(Eu)) and the mixture was stirred magnetically for 1 h at room temperature. After homogenisation, the mixture placed in an open Pyrex glass vial (20 mL capacity) was heated in an oven already preheated at 400 ºC. The oven was allowed to cool down at room temperature slowly (-20 $ºC \times h^{-1}$), taking approximately 19 h of reaction. After the thermal treatment, the black mixture has undergone a significant volume decrease. This residue is diluted with acetonitrile (0.5 mL) and was submitted to purification by silica gel column chromatography using as eluent acetonitrile that contained an increasing proportion of methanol for 0 to 50 %. The eluted fluorescent fraction was collected and the solvent removed under reduced pressure to obtain a viscous oil (between 50 and 70 mg) corresponding C-NOR and C-NOR(Eu) depending on the absence or the presence of $Eu(OAc)_3$ during the synthesis.

Characterisation techniques. HR-TEM images were taken with a JEOL 200 kV model JEM2100F. Images were analysed with INOVA software to determine sample particle, size distribution and interlayer distance. Particle size distribution was determined by measuring the dimensions of more than oine hundred nanoparticles from at least three independent batches. AFM measurements were carried out by using a Veeco AFM Multimodel instrument. ^{1}H- and ^{13}C-NMR spectra of C-NOR suspended in D_2O were recorded with Varian Genesis 300 MHz spectrometer. Particle size distribution of C-NOR and C-NOR(Eu) suspended in H_2O were determined using Malvern ZetaSizer Nano-ZS after appropriate dilution of the suspension at 25 ºC at a count rate of 53 and 388 KHz. The same instrument provides also the Z-potential value of both suspensions. The quality of these measurements was always good according to instrument parameters.

Cell Culture. Experiments were performed with the human cervical carcinoma cell line Hep3B. Reagents employed in cell culture were purchased from GIBCO (Invitrogen, Eugene, OR, USA). Hep3B cells were cultured in DMEM with a high glucose concentration (4.5 mg mL^{-1}). Hep3B culture media were supplemented with 10% heat-inactivated FBS, penicillin (50 units mL^{-1}) and streptomycin (50 µg mL^{-1}). Cells were maintained in an incubator (IGO 150, Jouan, Saint-Herblain Cedes, France) at 37 ^{o}C in a humidified atmosphere of 5% CO_2 + 95% air (AirLiquide).

Viability. Biocompatibility was assessed by MTT (3-[4,5-dimethylthiazol-2-yl]-2,5-diprenyltetrazolium bromide) test which is a colorimetric assay based on the ability of cells to reduce a soluble yellow tetrazolium salt to blue formazan crystals. This reduction takes place only when mitochondrial reductase enzymes are active and is, thus, a marker of cell viability related to mitochondrial function. For these experiments, cells were seeded in 96-well plates (Falcon, BD) at 10000 cells/well for Hep3B. Treatment was performed over 3 h. Then the medium was refreshed and cells were further cultured until a total of 24 h period. MTT reagent (Roche Diagnostics, Mannheim, Germany) was added (20 µL/well) for the last 4 h of the treatment. Cells were solubilised with DMSO (100 µL/well, 5 min, 37 ^{o}C) and the absorbance was measured using a "Multiscan" plate-reader spectrophotometer (Thermo Labsystems, Thermoscientific, Rockford, IL, USA). Results were obtained subtracting the absorbance at 690 nm-background absorbance from the 570 nm absorbance, as indicated in the instructions provided with the kit.

Confocal Fluorescence microscopy. These experiments were performed in Hep3B cells, seeded at 10000 cells/well in Nunc 8-well coverslip bottom chamber slides. Treatment with C-NOR or C-NOR(Eu) was performed over 24 h at 20 µg/mL in high glucose Dulbelcco's Modified Eagle Medium (Gibco) supplemented with 10 % Fetal Bovine Serum (Gibco), 100 U/mL penicillin, 100 µg/mL streptomycin (Gibco) and 2mM L-glutamine (Gibco). After that, the medium was removed, the cells were washed twice with HBSS (Sigma) and then cells were further incubated for 30 min at room temperature with 2.5 µM Hoescht (Molecular Probes), a blue fluorescent marker which preferentially stains nucleic acids. Then, the cell culture was washed with HBSS twice and immediately monitored by the microscopy. Confocal images were acquired using a Leica TCS-SP2 confocal laser scanning unit equipped with argon and Helium-Neon laser beams and attached to a Leica DM1RB inverted microscope. The excitation wavelengths for fluorochromes were 351 and 364 nm for Hoechst and 488 nm for C-NOR or C-NOR(Eu) samples and the emission apertures for fluorescence detection were 400–470 nm for Hoechst and 507–610 nm for C-NOR or C-NOR(Eu). The Z-section series were obtained by progressing from top to bottom in 1.18 ± 0.2 µm increments.

Conclusions

The present study shows that heating PTA at 400 ºC in low molecular mass PEG is a simple and reliable procedure leading to the self assembling and esterification of these molecules forming flat nanoobjects having a morphology of onion rings constituted by a stack of aromatic molecules. These nanoparticles can be purified by silica gel chromatography to obtain fractions with a very homogeneous particle size of about 35 nm measured by TEM. These C-NOR are highly fluorescent, the highest emission quantum yield measured upon excitation at 420 nm was 49%. The influence of Eu^{3+} in the thermal treatment is to favour the formation of these nanoobjects by acting as Lewis acid, probably promoting esterification between carboxylic acid groups and PEG. These nanoonion rings are highly biocompatible with Hep3B cells and can cross cell membrane.

In the context of the current intense research on the preparation of C-dots, our report shows a protocol for the preparation of structured carbon nanoobjects having a very well defined morphology. At the present the structure of most of the C-dots is ill-defined with not complete understanding of the structure of the emission sites. In contrast, nanoforms reported in the present work exhibit a well defined structure and morphology in which the molecular structure of a condensed polycyclic aromatic has been essentially preserved. The nanoobjects have well-defined onion ring morphology at the nanoscale having interesting fluorescence properties and biological compatibility, different from the properties of the precursor molecule. Thus, our result could in principle open new strategies for the development emitting carbon nanoforms based on aromatic molecules in PEG.

Acknowledgements.

Financial support by the Spanish Ministry of Economy and Competitiveness (Severo Ochoa and CTQ2012-32315) and Generalidad Valenciana (Promoteo 2012-013) is gratefully acknowleged. JRH and VMV are recipients of contracts from

Valencian Regional Government, the Ministry of Health (CP13/00252) and Carlos III Health Institute (PI13/1025), respectively. HGB and JRH thank the Generidad Valenciana and FIS for a postgraduate scholarship and a research contract, respectively.

Notes and references.

[a] Instituto Universitario de Tecnología Química CSIC-UPV and Departamento de Química, Univ. Politecnica de Valencia, Av. De los Naranjos s/n, 46022 Valencia, Spain
[b] Service of Endocrinology. University Hospital Dr. Peset, Foundation for the Promotion of Health and Biomedical Research in the Valencian Region (FISABIO), Valencia, Spain
[c] Institute of Health Research INCLIVA, University of Valencia, Valencia, Spain
[d] Department of Physiology, University of Valencia, Valencia, Spain
[e] Center of Excellence in Advanced Materials Research, King Abdulaziz University, Jeddah, Saudi Arabia

(1) Sun, Y. P.; Zhou, B.; Lin, Y.; Wang, W.; Fernando, K. A. S.; Pathak, P.; Meziani, M. J.; Harruff, B. A.; Wang, X.; Wang, H. F.; Luo, P. J. G.; Yang, H.; Kose, M. E.; Chen, B. L.; Veca, L. M.; Xie, S. Y. *Journal of the American Chemical Society* **2006**, *128*, 7756-7757.
(2) Baker, S. N.; Baker, G. A. *Angew. Chem., Int. Ed.* **2010**, *49*, 6726-6744, S6726/1-S6726/5.
(3) Liu, J.-H.; Yang, S.-T.; Chen, X.-X.; Wang, H. *Curr. Drug Metab.* **2012**, *13*, 1046-1056.
(4) Luo, P. G.; Sahu, S.; Yang, S.-T.; Sonkar, S. K.; Wang, J.; Wang, H.; LeCroy, G. E.; Cao, L.; Sun, Y.-P. *J. Mater. Chem. B* **2013**, *1*, 2116-2127.
(5) Luo, P. G.; Yang, F.; Yang, S.-T.; Sonkar, S. K.; Yang, L.; Broglie, J. J.; Liu, Y.; Sun, Y.-P. *RSC Adv.* **2014**, *4*, 10791-10807.
(6) Wang, Y.; Hu, A. *J. Mater. Chem. C* **2014**, *2*, 6921-6939.
(7) Fan, R.-J.; Sun, Q.; Zhang, L.; Zhang, Y.; Lu, A.-H. *Carbon* **2012**, *71*, 87-93.
(8) Jaiswal, A.; Ghosh, S. S.; Chattopadhyay, A. *Chem. Commun. (Cambridge, U. K.)* **2013**, *48*, 407-409.
(9) Kong, W.; Liu, R.; Li, H.; Liu, J.; Huang, H.; Liu, Y.; Kang, Z. *J. Mater. Chem. B* **2014**, *2*, 5077-5082.
(10) Mitra, S.; Chandra, S.; Pathan, S. H.; Sikdar, N.; Pramanik, P.; Goswami, A. *RSC Adv.* **2014**, *3*, 3189-3193.
(11) Lai, C.-W.; Hsiao, Y.-H.; Peng, Y.-K.; Chou, P.-T. *J. Mater. Chem.* **2012**, *22*, 14403-14409.
(12) Sachdev, A.; Matai, I.; Kumar, S. U.; Bhushan, B.; Dubey, P.; Gopinath, P. *RSC Adv.* **2013**, *3*, 16958-16961.
(13) Selim, K. M. K.; Xing, Z.-C.; Choi, M.-J.; Chang, Y.; Guo, H.; Kang, I.-K. *Nanoscale Res. Lett.* **2014**, *6*, 528/1-528/9.
(14) Lopez, C.; Zougagh, M.; Algarra, M.; Rodriguez-Castellon, E.; Campos, B. B.; Esteves da Silva, J. C. G.; Jimenez-Jimenez, J.; Rios, A. *Talanta* **2015**, *132*, 845-850.
(15) Ma, Y.; Wang, L.; Shao, J.; Tian, H. *Current Organic Chemistry* **2007**, *11*, 559-576.
(16) Yu, G. X.; Zhou, X. L.; Li, C. L.; Chen, L. F.; Wang, J. A. *Catalysis Today* **2009**, *148*, 169-173.
(17) Matthews, L. R.; Knobbe, E. T. *Chem. Mater.* **1993**, *5*, 1697-700.
(18) Pandya, S.; Yu, J.; Parker, D. *Dalton Trans.* **2006**, 2757-2766.
(19) Werts, M. H. V.; Jukes, R. T. F.; Verhoeven, J. W. *Phys. Chem. Chem. Phys.* **2002**, *4*, 1542-1548.
(20) Davydov, V. A.; Rakhmanina, A. V.; Agafonov, V.; Thorel, A.; Boudou, J. P. *Fullerenes, Nanotubes, Carbon Nanostruct.* **2006**, *14*, 425-428.
(21) Davydov, V. A.; Rakhmanina, A. V.; Boudou, J. P.; Thorel, A.; Allouchi, H.; Agafonov, V. *Carbon* **2006**, *44*, 2015-2020.
(22) Bogdanov, K.; Fedorov, A.; Osipov, V.; Enoki, T.; Takai, K.; Hayashi, T.; Ermakov, V.; Moshkalev, S.; Baranov, A. *Carbon* **2014**, *73*, 78-86.
(23) Kuznetsov, V. L.; Chuvilin, A. L.; Butenko, Y. V.; Mal'kov, I. Y.; Titov, V. M. *Chemical Physics Letters* **1994**, *222*, 343-348.
(24) Dubitsky, G. A.; Serebryanaya, N. R.; Blank, V. D.; Skryleva, E. A.; Kulnitsky, B. A.; Mavrin, B. N.; Aksenenkov, V. V.; Bagramov, R. K.; Denisov, V. N.; Perezhogin, I. A. *Russian Chemical Bulletin* **2011**, *60*, 413-418.
(25) Borgohain, R.; Yang, J.; Selegue, J. P.; Kim, D. Y. *Carbon* **2014**, *66*, 272-284.
(26) Hou, S.-S.; Chung, D.-H.; Lin, T.-H. *Carbon* **2009**, *47*, 938-947.
(27) Pervolaraki, M.; Komninou, P.; Kioseoglou, J.; Othonos, A.; Giapintzakis, J. *Appl. Surf. Sci.* **2013**, *278*, 101-105.
(28) Xiu, Y.; Gao, Q.; Li, G.-D.; Wang, K.-X.; Chen, J.-S. *Inorganic Chemistry* **2010**, *49*, 5859-5867.
(29) Zhu, S.; Meng, Q.; Wang, L.; Zhang, J.; Song, Y.; Jin, H.; Zhang, K.; Sun, H.; Wang, H.; Yang, B. *Angewandte Chemie-International Edition* **2013**, *52*, 3953-3957.
(30) Ignatius, A. A.; Claes, L. E. *Biomaterials* **1996**, *17*, 831-9.
(31) Marques, A. P.; Reis, R. L.; Hunt, J. A. *Biomaterials* **2002**, *23*, 1471-1478.
(32) Sung, H.-W.; Huang, R.-N.; Huang, L. L. H.; Tsai, C.-C. *J. Biomater. Sci., Polym. Ed.* **1999**, *10*, 63-78.